Video Article

Intermediate Strain Rate Material Characterization with Digital Image Correlation

Meysam Rahmat[1], David Backman[1], Richard Desnoyers[1]

[1]Aerospace Research Centre, National Research Council Canada

Correspondence to: Meysam Rahmat at Meysam.Rahmat@nrc-cnrc.gc.ca

URL: https://www.jove.com/video/59168
DOI: doi:10.3791/59168

Keywords: Mechanical characterization, dynamic, tensile, digital image correlation, high-speed servo-hydraulic load frame, stress, strain

Date Published: 11/30/2018

Citation: Rahmat, M., Backman, D., Desnoyers, R. Intermediate Strain Rate Material Characterization with Digital Image Correlation. *J. Vis. Exp.* (), e59168, doi:10.3791/59168 (2018).

Abstract

The mechanical response of a material under dynamic load is typically different than its behavior under static conditions; therefore, the common quasistatic equipment and procedures used for material characterization are not applicable for materials under dynamic loads. The dynamic response of a material depends on its deformation rate and is broadly categorized into high (i.e., greater than 200/s), intermediate (i.e., 10−200/s) and low strain rate regimes (i.e., below 10/s). Each of these regimes calls for specific facilities and testing protocols to ensure the reliability of the acquired data. Due to the limited access to high-speed servo-hydraulic facilities and validated testing protocols, there is a noticeable gap in the results at the intermediate strain rate. The current manuscript presents a validated protocol for the characterization of different materials at these intermediate strain rates. Strain gauge instrumentation and digital image correlation protocols are also included as complimentary modules to extract the utmost level of detailed data from every single test. Examples of raw data, obtained from a variety of materials and test setups (e.g., tensile and shear) is presented and the analysis procedure used to process the output data is described. Finally, the challenges of dynamic characterization using the current protocol, along with the limitations of the facility and methods of overcoming potential problems are discussed.

Introduction

Most materials demonstrate some degree of strain rate dependency in their mechanical behavior[1] and, therefore, mechanical testing conducted only at quasistatic strain rates is not suitable to determine the material properties for dynamic applications. The strain rate dependency of materials is typically investigated using five types of mechanical testing systems: conventional screw drive load frames, servo-hydraulic systems, high-rate servo-hydraulic systems, impact testers, and Hopkinson bar systems[1]. Split Hopkinson bars have been a common facility for the dynamic characterization of materials for the past 50 years[2]. There have also been efforts to modify Hopkinson bars to test at intermediate and lower strain rates. However, these facilities are typically more suitable for the high strain rate characterizations of the material (i.e., usually greater than 200/s). There is a gap in the literature on the strain rate characterization of material properties at intermediate strain rates in the range of 10−200/s (i.e., between quasistatic and high strain rate results obtained from split Hopkinson bars[3]), which is due to the limited access to facilities and a lack of reliable procedures of intermediate strain rate material testing.

A high-speed servo-hydraulic load frame applies load to the specimen at a constant and predefined velocity. These load frames benefit from a slack adaptor, which, in tensile tests, allows the crosshead to reach the desired velocity before the loading starts. The slack adaptor allows the head to travel a certain distance (e.g., 0.1 m) to reach the target velocity and then starts applying the load to the specimen. High-speed servo-hydraulic load frames typically perform tests under displacement control mode and maintain a constant actuator velocity to produce constant engineering strain rates[3].

Techniques for measuring specimen elongation are generally classified as either contact or noncontact techniques[4]. Contact techniques include the use of instruments such as clip-on extensometers, while laser extensometers are employed for noncontact measurements. Since contact extensometers are prone to inertia influences, they are not suitable for dynamic tests; noncontact extensometers do not suffer from this problem.

Digital image correlation (DIC) is an optical, non-contact, full-field strain measurement technique, which is an alternative approach to strain gauging to measure strain/load and overcome some of the challenges (e.g., the ringing phenomenon) associated with dynamic material characterization[5]. Resistance strain gauges can suffer from limitations such as a limited area of measurement, a limited range of elongation, and limited mounting methods, whereas DIC is always capable of providing a full-field strain measurement from the specimen surface during the experiment.

The presented procedure describes the use of a high-speed servo-hydraulic load frame along with DIC and can be used as a complementary document to the recently developed standard guidelines[6] to clarify the details of the experimental procedure. The section on the servo-hydraulic load frame can be followed for a variety of test setups (e.g., tensile, compressive, and shear) and even with common quasistatic load frames as well, and, therefore, covers a vast range of facilities. Furthermore, the DIC section may be applied separately to any type of mechanical or thermal tests, with minor modifications.

Copyright © 2018 Journal of Visualized Experiments

Protocol

1. Specimen preparation

1. Prepare dog bone shaped tensile specimens according to ISO standard[6] in advance.
   NOTE: Similar specimens are also used[4].
2. Install strain gauges on the tab section (mandatory for load measurement) and on the gauge section (optional for strain measurement) of the tensile specimen.
   1. Select the proper model of strain gauge based on the size, maximum extension, testing temperature, electrical resistance, etc.[4].
   2. Clean the surface of the specimen with isopropanol to remove any contamination and install the strain gauge at the proper location. Install the tab section strain gauge at equal to or greater than the width of the tab section from the gripping section and the gauge section to ensure a uniform stress flow of the nominal value (i.e. no stress concentration), otherwise the numerical analysis is required to predict the stress value at the location of the strain gauge.
   3. Connect the strain gauge wires to the Wheatstone bridge box. Use a wire connection tab if required to mount the connections to the external wires.
   4. Verify the strain gauge reading with a simple loading and boundary conditions. Apply a known load to the specimen (e.g. hang a known mass from the specimen) and check the strain readouts.
3. Prepare the specimen for DIC as follows:
   1. Prepare the surface of the specimen with high contrast features. For example, paint the specimen white and speckle it with fine black dots. Through trial and error match the speckle pattern to the camera image sensor size such that each speckle is composed of approximately 3 pixels or more.
      NOTE: Avoid performing DIC on the side that the strain gauges are installed to prevent the undesirable surface features.
   2. Leave the paint to dry before the test. Test the specimen, preferably, in the same day it was painted.
      NOTE: Depending on the type and consistency of the paint, this may take up to a few hours. Do not leave the speckled specimens for a prolonged period (e.g., several days) before testing as this will result in the paint becoming brittle and flaking off during the test.

2. Start-up procedure

1. Turn on the power to the Control Console using the button on the UPS (Uninterruptable Power Supply). Check that the isolation valve from the pump to the High Rate frame is open, and then turn on the computer.
2. From the desktop start the Controller Application, selecting the **High Rate Calculate Displacement.cfg** configuration, then click **Reset** to clear interlock 1 (under **Station Controls**).
   NOTE: The other two indicators (**Program 1** and **Gate 1**) will be red because the high pressure hydraulic is not applied yet.
3. Check **Exclusive Control** so the frame can only be controlled from the software (and not from the handset).
4. Now, start up the hydraulic pump (HPU) and open the service manifold (HSM 1) one by one (3 total). For each case wait until the low indicator stops flashing before pressing the high indicator. If the pump has been off for a long time, wait for 30 s before selecting the high to give the feeder pump time to supply oil to the high-pressure pump.
5. Again, from the desktop, start the Test Design software. From the toolbar make sure the HPU and HSM 1 are **ON** (green). From the top menu **File> New> Test from Template** select **Custom Templates**, and then select **Tension test**.

3. Setup of the strain gauges

1. Go to the load frame crosshead control (next to the handset) and turn the switch to the low rate (**turtle icon**).
2. Inside the test chamber connect the wires of the specimen strain gauge(s) to the strain gauge box using the color code (red, white and black). If there is only one strain gauge, use the SG 1 series.
   NOTE: The red lead is the separate terminal (excitation + or -), and the white and black are the sense and signal leads.
3. In the Controller Application and under **Auxiliary Inputs** go to Strain 1 (or 2) to select the maximum range of the strains (i.e. 2%, 5%, or 10%). For example, if 5% is chosen, the software maps this from 50,000 με to 10 Volts output and cannot measure strains beyond 5%.
4. Run the Conditioner Utility software to configure the strain gauges and balance the Wheatstone bridge according to the following steps:
   1. Calculate the output voltage using the formula for the Wheatstone bridge:

      $$V_O = \frac{1}{4} V_E GF(\varepsilon_1 - \varepsilon_2 + \varepsilon_3 - \varepsilon_4) \times 10^{-6}$$

      Here, V_O is the output voltage, V_E is the excitation voltage, GF is the gauge factor, ε_1 is 50,000 (5%), whereas ε_2, ε_3, and ε_4 are zero (completion bridge).
5. Calculate the gain using the following equation:

   $$Gain = \frac{Excitation\ Voltage}{Output\ Voltage} = \frac{V_E}{V_O}$$
6. In the conditioner utility software, there are options of 1, 8, 64, and 512 for the Preamp Gain, while the Post amp Gain value is limited to 9. 9976. Calculate the Post amp Gain based on different options of 1, 8, 64, and 512 for the Preamp Gain using the following equation:

   $$Post\ amp\ Gain = \frac{Gain}{Preamp\ Gain}$$

7. Select the lowest Preamp Gain that gives out a Post amp Gain that is lower than 9.9976 and input these values into the conditioner utility software.
8. Run the High Rate Data Acquisition Configuration software. Under the strain channels (Channel 3 and 4), enter the full-scale range of the strain gauge (e.g. 50,000).
   NOTE: Channel 1 and 2 are dedicated to Displacement and Force, respectively.
9. Offset the strain gauges to zero according to the following steps:
   1. First in the software, remove any offset values for the strain channels (bring offset values to zero).
      NOTE: This process has to be done when the test specimen is resting (e.g. on the table) and is not under load.
   2. Then, adjust the **Bridge balance** parameter to bring the readout strain almost to zero. This is the coarse adjustment step.
   3. Then adjust the **Feedback Zero** parameter, to bring the strain value in the strain manager software completely to zero. This step is the fine adjustment.
   4. To assure the input parameters were correct, click on **Shunt Enable** option.
      NOTE: The strain value in the Controller Application software should read 1640 με (with either + or - sign). Remember to turn off the shunt to remove the shunt resistor out of the Wheatstone bridge. The Strain value will go back to zero.
10. If there are two strain gauges on the specimen, in theconditioner utility software, click on **Strain 2** and repeat all the strain gauge setup steps.

4. Mounting the test specimen

1. In the Controller Application activate the **Manual Control** and enter the position of the head to full extension at -125 mm.
2. Then click to turn off the **Enable Manual Command** check box and uncheck the **Exclusive Control** box.
3. Use the mounting fixture to align the coupon inside the grips. An elastic cord may be used to hold the slack adapter in a retracted position giving room to install the coupon. Tighten the coupon in the bottom grip first.
4. On the handset push the **key** icon on the top right corner to activate the handset. Ensure that the **Exclusive Control** box on the software is unchecked. Make sure the top grip is loose to prevent the undesirable application of load to the specimen.
   1. Remove the elastic cord and push the **wheel** icon below the thumbwheel on the controller to activate it. Slowly roll the wheel to bring the head down until the bottom arm of the slack adaptor is almost fully retracted and the crosshead is nearly at -125 mm.
      NOTE: the position of the head can be read on the handset.
5. On the handset push the **key** icon once again to de-activate the handset. Return to the computer and on the Controller Application check the **Exclusive Control** box and use the **Manual Control** to bring the head to exactly -125 mm. The top grip is loose so there is no load applied to the coupon.
6. Now, tighten the top grips with a wrench and a key by rotating the slack adapter. Do not twist the coupon while tightening the grip.
7. Check the spiral washers (i.e. a very shallow spiral) between the slack adaptor and the intermediate crosshead and make sure they are tight and there is no axial clearance along the load train.
8. Again, using the crosshead control box return the frame to the high rate (rabbit icon), and make sure the enclosure doors are tightly closed.
9. Back on the computer, to clear the interlocks click **Reset** (on the right-hand side of the Controller Application).
   NOTE: The interlocks include "Interlock 1" (an interlock chain running through all frames and the hydraulic pump), "Program 1" (computer software controlled, for example, high/low velocity), "Gate 1" (enclosure and Rate switch), and "C-Stop 1" (controlled stop).
10. When there is no intention to move the head manually, uncheck the **Enable Manual Command** box in **Manual Command** menu to avoid accidentally entering a number into the software and moving the head.

5. DIC setup preparation

1. Connect the high-speed camera to the computer using a Gigabit LAN Cable.
2. Connect the Digital I/O box to the high-speed camera and MTC frame controller.
3. Connect the computer to the MTS frame controller through the DAQ box. Force and displacement signals are transferred from the MTS controller to the computer through this box.
4. Connect the high-speed camera to the DAQ box for the trigger signal and the synchronization signal.
5. Mount the camera onto the base of the load frame to avoid relative movement between the camera and specimen during the test, as the frame shakes due to the impact.
6. Position the camera carefully to ensure its image sensor is parallel to the specimen. Use a telecentric lens (e.g., Opto-engineering 23-64with a field of view of 64 × 48 mm and a working distance of 182 mm) to reduce the possibility of perspective distortion from out-of-plane motion.
7. During camera setup, consider the final deformation of the specimen and make sure the camera's field of view covers the specimen throughout the entire test.
8. To set up the software connections in the computer, select **Network and Sharing Centre** from Windows **Control Panel**. Next click Local Area Connection.
9. Select **Internet Protocol Version 4 (TCP/IPv6)** in the **Local Area Connection** properties and set the IP address.
10. Open the High-Speed Imaging viewer software and click detect and then save the setup.
11. Click on the **Camera Option** button and select the I/O tab to set the external signals.
12. To set the frame rate and frame resolution, click on the **variable** button. Set the camera frequency and the data acquisition (DAQ) box acquisition rate to the same number as the high-speed data acquisition system in the load frame to make the data analysis step easier
13. **Open** the high speed DAQ in the High-Speed Imaging viewer and select the required channels and the samples per frame.
14. After camera setup, capture several static images and calculate the strain field using the image correlation routine.
    NOTE: The maximum strain and displacements measured from this noise floor are noted and provide a qualitative measure of the image quality.

6. Running the test

1. In the test design software, from the top menu follow **File> New> Test> Test from Template**. Then under **Custom Templates** open **Tension Test**.
2. Select **New Test Run** and enter a valid file name (usually the name of the coupon without spaces). Modify the fields as needed; then click **OK**.
    1. If strain gauges are included, remember to input **Channel Count** as 4.
    2. The starting point is usually -125 mm. This is important because if this is not correct the head will move to this value before the test starts possibly damaging the coupon.
    3. The default values for **High Speed Acquisition Rate** and **Buffer Size** are 50,000 and 20,000, respectively. Depending on the duration of the test and required time resolution (time interval between data points), modify these numbers if necessary.
    NOTE: The default parameters result in saving data for the duration of 0.4 s.
    4. For **Ramp Rate** select the nominal desired head velocity (for example, 8,000 mm/s), then click **OK**.
3. A series of prompts will appear, reminding to check key hardware times, after which the test will be initiated by clicking on the **Run** icon.
4. On the Control Console switch the **Mode Select** to **High Rate**. This activates the large valve for high rate load application. The default **Valve 1** is selected (the light is on).
5. On the computer screen, a series of steps are shown. Follow the steps.
6. On the Control Console, depress and hold **Arm/Charge Accumulator** switch. The system is now ready.
7. Press **Fire** to complete the test.
8. Switch the **Mode Select** back to **Standard** and press the **return to start** (Green button) on the console to return the head back from the endcap (125 mm).
9. Go to the crosshead control and switch back to the low rate (turtle icon).
10. Open the enclosure and take out the specimen. Find the data files stored on the computer at C:\Datafiles\High Rate Data (for high rate data) and at C:\Datafiles\Low Rate Data (for low rate data).

7. Shutdown procedure

1. On the Controller Application software turn the HSM 1 to **Low** (yellow) and then to **Off** (red). This will close the manifold and shut down the pump.
2. In the test design software, save the test run, if required, by following from the top menu **File> Save** as and then choose the test. Close the test design software.
3. Close the Controller Application. Save the parameters before closing the software, if required. Shut down the computer.
4. Close the hydraulic valve (large lever) and turn off power to the Control Console again using the power button on the UPS.

8. Data analysis

1. Export the raw data from the load frame computer into the post-processing software of choice.
2. Calculate the actual load from the strain gauge readouts mounted on the gauge section and compare it with the raw load data from the high speed DAQ. If the ringing in the high speed DAQ data is severe, use the calculated load from the strain gauge in the next steps[4].
3. Calculate the stress in the gauge section, σ_{gauge}, based on the calculated load, P, and the specimen cross-section at the gauge section, $A_{x\text{-}section}$:
$$\sigma_{gauge} = \frac{P}{A_{X-section}}$$
4. Obtain the strain on the gauge section from one of the following methods:
    1. Average strain in the gauge section:
        1. Calculate the tab section elongation by knowing the load, tab section length, specimen's elastic modulus, and cross-sectional area.
        NOTE: If the elastic modulus is a function of strain rate, an iterative procedure (details are explained in reference[7]) is required.
        2. Subtract the tab section elongation from the entire specimen elongation (i.e. load frame head displacement) to obtain the gauge section elongation.
        3. Calculate the average strain in the gauge section based on the gauge section elongation and the initial length.
    2. Local strain from DIC:
        1. Determine the location on the gauge section where the specimen failed (i.e. split in two) and restrict the strain field to a local area at the vicinity of the failure section.
        2. Measure and record the strain in the local area using the DIC post-processing software of the choice.
5. Draw the stress-strain curve obtained from the previous steps.

Representative Results

The duration of a dynamic test is typically comparable to the time required for the stress waves to travel a round trip over the length of the load train (i.e. grips, specimen, and loading) system[1]. A dynamic test is valid if the number and amplitude of stress waves during a dynamic test is controlled so that a dynamic equilibrium is achieved, and the specimen experiences a homogeneous deformation at an almost constant strain rate. The Society of Automotive Engineers (SAE) draft SAE J2749 standard[8] calls for at least 10 elastic reflected waves to propagate through the specimen gauge length prior to the specimen yield point. Higher natural frequency systems usually have ringing oscillations (i.e. oscillations of the signal, usually in response to a step input) with lower amplitudes. This ringing phenomenon is the main challenge in a dynamic test at medium to high strain rates. The level of ringing (i.e. frequency and amplitude of the oscillating signal) determines whether the raw load data obtained from the load frame are acceptable or not. **Figure 1** shows examples of the load signals for two different tests. In both tests, the load obtained from the load frame is compared to the load calculated based on the strain gauge output installed on the tab section of the specimens. Although both these tests were performed properly, the load data directly extracted from the load frame force link cannot be used for the case shown in **Figure 1b**. In this case, using an alternative load measurement technique, such as tab section strain gauging, is necessary; whereas, the raw load data from the load frame (shown in **Figure 1a**) has good agreement with the strain gauge loads. In such cases, further tests may be performed without installing tab section strain gauges and the load can be directly read from the load frame force link. The ringing phenomenon has been previously observed by other researchers[3,9,10,11]. The amplitude and frequency of the oscillations are determined based on parameters such as the specimen material, geometry, and strain rate, and when the combination of all these factors leads to minor ringing, the raw data is used directly or, if necessary, after applying minor smoothing techniques such as filtering.

A typical example of DIC results for a dogbone aluminum specimen is shown in **Figure 2**. The strain field evolution with time on the entire gauge section is shown in this figure. The specimen was fixed at the bottom grip, and the top grip applied tension. In this test, the high-speed camera had a frame rate of 50,000 Hz and captured around 100 images during the test, but the images shown in this figure are 0.4 ms apart. The uniform strain within a given cross-section of the specimen shows the proper loading and data analysis during the test. The loss of DIC correlation in the last image was due to severe necking, which resulted in paint flaking, and was unavoidable immediately before the failure at the vicinity of the failure zone.

Figure 3 illustrates the stress-strain curves obtained from DIC and from the load frame crosshead displacement data. This figure shows the average stress-strain in the entire gauge section and is only presented to demonstrate the validity of the techniques and the good agreement between the results. When studying the local necking in the gauge section through DIC, the results cannot be compared with the average strains obtained over the entire gauge section. During the necking phenomenon, most of the deformation occurs at the necking region and the rest of the gauge section does not stretch but moves almost as a rigid body. Therefore, when calculating the average strain over the gauge section, this local stretch in the necking area is assigned to the entire gauge section with a longer length, compared to the length of the necking zone, and will result in a lower failure strain.

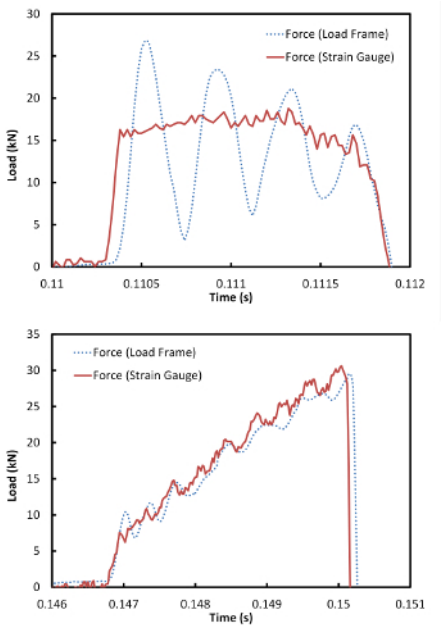

Figure 1: Comparison of load obtained from the load frame force link and calculated from the strain gauge. The ringing phenomenon in the force link data (dotted blue line) for case (A) is acceptable and for case (B) is not acceptable. Panels (A) and (B) show examples of experimental results for two tests with different samples (e.g. material, dimension, etc.) and strain rate. In each figure, the load data obtained from the load frame (dotted blue) and calculated from strain gauge readouts (solid red) are illustrated. The minor level of oscillation (i.e. ringing) in the load frame data in panel (A) demonstrates that this test does not require strain gauge instrumentation, but the severe ringing shown in panel (B) makes the strain gauge instrumentation necessary. Please click here to view a larger version of this figure.

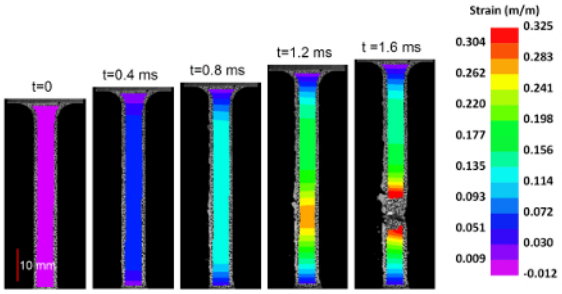

Figure 2: Strain field in the gauge section of an aluminum dogbone specimen during the test. The strain values are in m/m and the images are 0.4 ms apart. The DIC results on the gauge section of a metallic dogbone specimen are shown in this figure. Five different snapshots (out of the 100 images taken) are presented to demonstrate the evolution of strain and specimen stretching with time. The legend of all images is also shown to define the strain level associated to each color. Please click here to view a larger version of this figure.

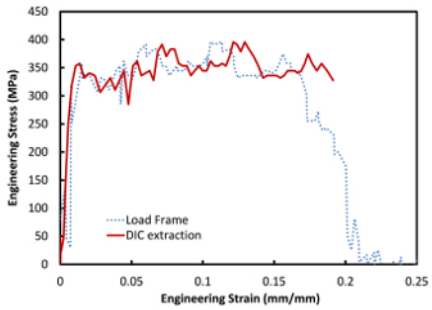

Figure 3: Comparison of the load frame and DIC extracted average stress-strain curves over the entire gauge section. The stress-strain curves determined from the load frame results (dotted blue) and extracted from DIC results (solid red) are shown here. Please click here to view a larger version of this figure.

Discussion

The raw data obtained from the experiment is influenced by the specimen geometry and strain gauges location on the specimen. The load data in low strain rate dynamic tests acquired by a piezo-electric load washer incorporated into the load frame at higher strain rates (Bruce *et al*.[3] suggested > 10/s, while for Wang *et al*.[9] reported this limit to be 100/s) typically suffer from large amplitude oscillations due to dynamic waves associated with the loading. As shown in **Figure 1a** combination of specimen material, geometry and strain rate may render the load washer signal impractical due to a high level of noise. Hence, alternative approaches of load reading must be considered, from which installing a strain gauge on the tab section of the specimen is the most common[3]. In order to calculate the load from the measured strain data, it is critical to ensure the tab section (where the load calculation strain gauge is installed) remains in the elastic deformation regime during the test. Also as explained in the protocol section, in order to ensure the absence of any boundary effects (i.e. due to the Saint-Venant's Principle) the strain gauges are required to be installed far from the grip section (where they are affected locally by load), or the gauge section (where a change in geometry disturbs the uniform flow of stress), otherwise finite element analysis are needed to compensate for the stress concentration factor[4]. During the data analysis step, employing a variety of filtering techniques, such as Fast Fourier Transformation (FFT) and averaging, in order to remove or reduce the noise level is also reported[12]. However, this approach runs the risk of possibly masking the yielding behavior and, therefore, is not recommended.

As the main challenge in intermediate strain rate mechanical tests, the ringing typically results from two main sources: the wave propagation, and system ringing[13]. Different researchers recommend allowing for more than three round trips[5,14] (10 round trips in the case of polymers[1,8]) of the stress waves through the gauge length in order to reach the dynamic equilibrium. For strain rates greater than 200/s, the test duration decreases to the order of 0.1 ms, which is comparable to three round-trip time and therefore bar systems (e.g. Hopkinson) are preferred over the servo-hydraulic load frames. The second source of load signal oscillation is related to the ringing phenomenon[1,14,15,16,17,18,19,20,21], which occurs when the impulse during load introduction leads the test system to oscillate due to inertia effects[22]. Employing lightweight clamps and mounting the specimen as close as possible to the force link will be effective to reduce the ringing effect[15,23] for strain rates below 100/s. The most dominant factor in reducing ringing is to improve the measurement technique as discussed extensively in the literature[3,9,10,11,16,17] where piezo-electric load washers (force links) were recognized as being unsuitable for strain rates beyond 100 s^{-1}, due to their lag and oscillations[3,15]. The common solution, as presented here, involved attaching strain gauges on the tab section of the specimen[1,3,9,10,11,16,17]. A post-test evaluation of the failed specimen should confirm that the specimen failure occurred at the gauge section, with no signs of slipping observed at the grip sections. The strain rate should also be evaluated to ensure it remained constant during a dynamic test[24].

Closed form solutions[1,11] or finite element analyses[10,25,26] have been employed by a variety of research groups to model intermediate to high strain rate tests. These studies help understand the physics of the phenomena in such tests as well as target specimen design and optimization to attain reliable results; however experimental procedure as explained herein are still the main source of material characterization data. Incorporating the material properties, obtained from such experimental investigations, into new simulations, the designer can model complicated dynamic failure scenarios, such as full-scale car crashes.

Disclosures

The authors have nothing to disclose.

Acknowledgements

The authors acknowledge the great assistance from Dmitrii Klishch, Michel Delannoy, Tyler Musclow, Joshua Ilse and Alex Naftel. Financial support by the National Research Council Canada (NRC) through the Security Materials Technology (SMT) Program is also appreciated.

References

1. Xiao, X., Dynamic tensile testing of plastic materials. *Polymer Testing.* **27** (2), 164-178 (2008).
2. Nemat-Nasser, S., Isaacs, J.B., Starrett, J.E., Hopkinson techniques for dynamic recovery experiments. *Proceedings of Royal Society of London A Mathematical Physical and Engineering Sciences.* **435**(1894), 371-391 (1991).
3. Bruce, D., Matlock, D., Speer, J., and De, A., Assessment of the strain-rate dependent tensile properties of automotive sheet steels. *SAE World Congress.* Detroit, United States (2004).
4. Rahmat, M., Dynamic mechanical characterization of aluminum: analysis of strain-rate-dependent behavior, *Mechanics Time-Dependent Materials.*, In Press (2018).
5. Gray, G. and W.R. Blumenthal, Split-Hopkinson pressure bar testing of soft materials. *ASTM International.* Vol. 8, Materials Park, OH, 1093-1114 (2000).
6. ISO, ISO 26203-2:2011; Metallic materials-Tensile testing at high strain rates-Part 2: Servo-hydraulic and other test systems. *International Organization for Standardization.* Switzerland, 15 (2011).
7. Rahmat, M. Naftel, A., Ashrafi, B., Jakubinek, M. B., Martinez-Rubi, Y., Simard, B., Dynamic Mechanical Characterization of Boron Nitride Nanotube - Epoxy Nanocomposites, *Polymer Composites.*, In Press (2018).
8. SAE, High strain rate testing of polymers. *SAE International.* 27 (2008).
9. Wang, Y., Xu, H., Erdman, D.L., Starbuck, M.J., Simunovic, S., Characterization of high-strain rate mechanical behavior of AZ31 magnesium alloy using 3D digital image correlation. *Advanced Engineering Materials.* **13**(10), 943-948 (2011).
10. Mansilla, Regidor, A., García, D., Negro, A., Dynamic tensile testing for determining the stress-strain curve at different strain rate. *6th International Conference on Mechanical and Physical Behaviour of Materials Under Dynamic Loading.* **10**(9), p. 695-700, Krakow, Poland (2000).
11. Zhu, D., Mobasher, B., Rajan, S.D., Peralta, P., Characterization of Dynamic Tensile Testing Using Aluminum Alloy 6061-T6 at Intermediate Strain Rates. *Journal of Engineering Mechanics.* **137**(10), 669-679 (2011).
12. Schossig, M., Bieroegel, C., Grellmann, W., Bardenheier, R., Mecklenburg, T. Effect of strain rate on mechanical properties of reinforced polyolefins. in *16th European Conference of Fracture.* Kluwer Academic Publishers, Alexandroupolis, Greece, 507-508 (2006).
13. Xia, Y., Zhu, J., Wang, K., Zhou, Q., Design and verification of a strain gauge-based load sensor for medium-speed dynamic tests with a hydraulic test machine. *International Journal of Impact Engineering.* **88,** 139-152 (2016).
14. Yang, X., L.G. Hector, and J. Wang, A Combined Theoretical/Experimental Approach for Reducing Ringing Artifacts in Low Dynamic Testing with Servo-hydraulic Load Frames. *Experimental Mechanics.* **54**(5), 775-789 (2014).
15. Xia, Y., J. Zhu, and Q. Zhou, Verification of a multiple-machine program for material testing from quasi-static to high strain-rate. *International Journal of Impact Engineering.* **86,** 284-294 (2015).
16. Yan, B., Kuriyama, Y., Uenishi, A., Cornette, D., Borsutzki, M., Wong, C. Recommended Practice for Dynamic Testing for Sheet Steels - Development and Round Robin Tests. *SAE International.* Detroit, United States (2006).
17. Borsutzki, M., Cornette, D., Kuriyama, Y., Uenishi, A., Yan, B., Opbroek, E. Recommendations, Recommendations for Dynamic Tensile Testing of Sheet Steels. *International Iron and Steel Institute.* Brussels, Belgium (2005).
18. Rusinek, A., Cheriguene, R., Bäumer, A., Klepaczko, J.R., Larour, P., Dynamic behaviour of high-strength sheet steel in dynamic tension: Experimental and numerical analyses. *The Journal of Strain Analysis for Engineering Design.* **43**(1), 37-53 (2008).
19. Diot, S., Guines, D., Gavrus, A., Ragneau, E., Two-step procedure for identification of metal behavior from dynamic compression tests. *International Journal of Impact Engineering.* **34**(7), 1163-1184 (2007).
20. LeBlanc, M.M. and D.H. Lassila, A hybrid Technique for compression testing at intermediate strain rates. *Experimental Techniques.* **20**(5), 21-24 (1996).
21. Xiao, X. Analysis of dynamic tensile testing. in *11th International Congress and Exhibition on Experimental and Applied Mechanics.* Orlando, United States, Society for Experimental Mechanics (2008).
22. Othman, R., Guégan, P., Challita, G., Pasco, F., LeBreton, D., A modified servo-hydraulic machine for testing at intermediate strain rates. *International Journal of Impact Engineering.* **36**(3), 460-467 (2009).
23. Kwon, J.B., Huh, H., Ahn, C.N., An improved technique for reducing the load ringing phenomenon in tensile tests at high strain rates. in *Annual Conference and Exposition on Experimental and Applied Mechanics.* Costa Mesa, United States, Springer New York LLC (2016).
24. Pan, W. and R. Schmidt. Strain rate effect in material testing of bulk adhesive. in *9th International Conference on Structures Under Shock and Impact.* The New Forest, United Kingdom, **87**, 107-116 (2006).
25. Zhang, D.N., Shangguan, Q.Q., Xie, C.J., Liu, F., A modified Johnson-Cook model of dynamic tensile behaviors for 7075-T6 aluminum alloy. *Journal of Alloys and Compounds.* **619**, 186-194 (2015).
26. Fitoussi, J., Meraghni, F., Jendli, Z., Hug, G., Baptiste, D., Experimental methodology for high strain-rates tensile behaviour analysis of polymer matrix composites. *Composites Science and Technology.* **65**(14), 2174-2188 (2005).

Copyright © 2018 Journal of Visualized Experiments